

SOLID-STATE PHYSICS

THE ELECTRONIC SPECTRUM AND OPTICAL TRANSITIONS IN SUPERLATTICES WITH QUASI-LOCALIZED STATES IN THE UNIT CELL

A. V. Dmitriev and V. V. Makeev

For a superlattice whose unit cell contained quasi-localized electron states, the electron spectrum structure was studied and the dipole matrix element of intersubband transitions was calculated. The dispersion relation and the band structure of such a superlattice were determined. The wave functions and the electron spectrum were found to possess peculiar hybrid properties near the energy corresponding to the quasi-localized state in an isolated quantum well. The absorption coefficient of the heterostructure in this region was substantially increased.

INTRODUCTION

It has long been a commonly accepted view that, in semiconductors, as in crystals in general, either the Bloch band electron states or the localized states in the forbidden band can only exist. However, in many circumstances, an important role is played by states of the third type, namely, the resonance or quasi-localized states [1]. These states, which have long been known in optics [2] and quantum mechanics [3], arise in semiconductors, for instance, when an impurity level split out from an allowed band occurs against the background of another band, or when a deep impurity level falls into the background of an allowed band. Under certain conditions, the resonance states may have a substantial influence on kinetic processes in semiconductors [4, 5].

Quasi-localized states may also arise in artificial semiconducting structures such as two-barrier structures. It has been shown in [6] that they distinctly manifest themselves in the optical properties of such structures and noticeably increase the coefficient of their intersubband absorption in the frequency range corresponding to the transition to the resonance state. Since this state formally belongs to the continuum and is delocalized, it can be expected that the observation of a contribution to photocurrent of an electron that underwent the transition into a quasi-localized excited state should not require the application of a strong electric field. This offers promise for the use of heterostructures with quasi-localized states in designing IR radiation receivers. Such receivers should feature a combination of the selectivity of absorption and the ability to operate at a weak dark current. This can be achieved at weak working electric fields. Such a combination is difficult to attain with traditional IR photodetectors based on heterostructures where there are used transitions either to a localized state or, conversely, to the continuum (see review [7]).

The properties of a virtually isolated quantum well were considered in [6]. At the same time, either bodies of quantum wells or superlattices are used in experimental studies and applications. It would therefore be interesting to study the properties of periodic structures comprised of quantum wells with resonance states. The elucidation of the special features of interactions between resonance states of different quantum

wells and between such states and the continuum under these conditions is of theoretical interest on its own. This problem is tackled in the present work.

The theoretical formalism for the calculation of the superlattice electron spectra is well developed (e. g., see [8, 9]). A detailed analysis of the spectrum of a traditional AB-type superlattice (two alternating layers) can be found in [10]. We will use a similar approach to analyze the spectrum of a superlattice with a more intricate unit cell structure.

1. MODEL

For definiteness, we consider one nondegenerate (conduction) band of a composite superlattice where each unit cell is described in terms of the effective mass method by the one-dimensional model potential (Fig. 1)

$$U(x) = \begin{cases} -V, & 0 < x < a \\ 0, & a < x < b \end{cases} + \Omega [\delta(x) + \delta(x - a)]. \quad (1)$$

Here, x is the direction of superlattice growth; a and b are the well width and the structure period, respectively; and V is the well depth. The δ -shaped barriers at the well boundaries are a simplified approximation to auxiliary finite-height and finite-thickness barriers surrounding each well, which, together with main barriers of thickness $(b - a)$, separate the wells. The reciprocal tunnel penetrability of these additional barriers is characterized by the Ω parameter. The energy in (1) is counted from the top of the main barrier.

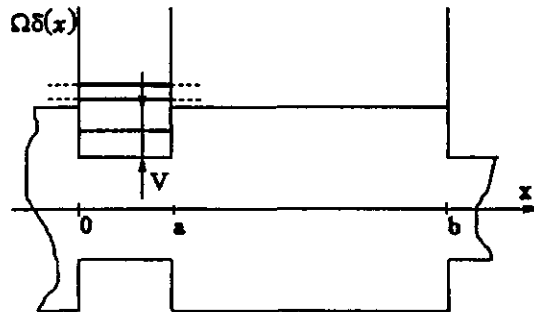


Fig. 1

Model potential. The positions of the lowest minibands are shown schematically.

If the whole structure had consisted of a single quantum well with potential (1), we might have spoken of the presence of quasi-localized states in its spectrum. These states arise close to the energies that would be characteristic of localized dimension-quantized states between the additional barriers surrounding the well if these barriers were impenetrable. The finite penetrability of these barriers transforms localized states lying above the main barrier into resonance states. In Fig. 1, they are shown by two upper levels in the well, whereas the lower level in an isolated well is localized.

Let us consider how the presence of resonance states in the wells affects the properties of the structure as a whole. The wave function envelopes in the heterostructure can be written in the form

$$\Psi(x) = \begin{cases} A_1 e^{iqx} + A_2 e^{-iqx}, & 0 < x < a; \\ B_1 e^{i\kappa x} + B_2 e^{-i\kappa x}, & a < x < b; \end{cases} \quad (2)$$

$$\Psi(x + b) = e^{ikb} \Psi(x),$$

where $q = (1/\hbar)\sqrt{2m(E + V)}$, $\kappa = (1/\hbar)\sqrt{2mE}$; E is the particle energy counted from the top of the main barrier; m is the effective mass; and kb is the phase shift of the envelope function corresponding

to the displacement by one superlattice period. Ignoring the difference of the effective masses between heterostructure layers and following the usual technique, we obtain the boundary condition at the well left-hand boundary ($x = 0$),

$$\begin{cases} \Psi(x)|_{0^-}^{0^+} = 0, \\ \frac{d}{dx} \ln \Psi(x)|_{0^-}^{0^+} = \Omega. \end{cases}$$

Imposing similar boundary conditions at the right-hand boundary ($x = a$), we obtain a system of equations for the coefficients of equation (2) determining the envelope function,

$$\begin{pmatrix} e^{ikb} & e^{ikb} & -e^{i\kappa b} & -e^{-i\kappa b} \\ (q + i\Omega) e^{ikb} & (-q + i\Omega) e^{ikb} & -\kappa e^{i\kappa b} & \kappa e^{-i\kappa b} \\ e^{iqa} & e^{-iqa} & -e^{i\kappa a} & -e^{-i\kappa a} \\ (-q + i\Omega) e^{iqa} & (q + i\Omega) e^{-iqa} & \kappa e^{i\kappa a} & -\kappa e^{-i\kappa a} \end{pmatrix} \begin{pmatrix} A_1 \\ A_2 \\ B_1 \\ B_2 \end{pmatrix} = 0.$$

The condition of zero determinant of the matrix of the coefficients in this equation gives the dispersion relation

$$\cos kb = \frac{\Omega^2 - q^2 - \kappa^2}{2\kappa q} \sin \kappa(b-a) \sin qa + \frac{\Omega}{q} \cos \kappa(b-a) \sin qa + \frac{\Omega}{\kappa} \sin \kappa(b-a) \cos qa + \cos \kappa(b-a) \cos qa. \quad (3)$$

The energy ranges where the magnitude of the right-hand side of (3) does not exceed unity correspond to the allowed minibands of our superlattice. Unfortunately, we have failed to obtain analytic expressions for the coefficients of wave function (2) at an arbitrary k value, and for this reason, further calculations were performed numerically.

2. RESULTS AND DISCUSSION

The wave functions for several neighboring minibands are shown in Fig. 2. The lower plot corresponds to the wave function of the lowest miniband formed from the ground state in the wells. Naturally, the electron density in the wells is largely concentrated in this miniband. The shape of the wave functions is almost independent of k within a well, and changes in k only cause changes in the phase shifts between the functions of neighboring unit cells.

The other wave functions in Fig. 2 have positive energies, which lie above the main barrier of thickness $(b-a)$ between wells. In most of them, the electron density is concentrated in the region between the wells; that is, these functions are constructed of electron states in the region of main barriers, where additional δ -barriers prevent particles from being transferred to the well region. Note that such functions corresponding to opposite miniband boundaries are characterized by different parities with respect to the center of the well.

The exceptions are the functions corresponding to the miniband located close to the energy of resonance states, which will be called the resonance miniband. In the states of this miniband, the electron density is high in the region of wells, and the states have equal parities at both miniband boundaries. Their structure resembles that of the functions of the lowest miniband formed from localized well states. It follows that the dipole matrix element of the transition from the lowest miniband to minibands located in the vicinity of the resonance should be anomalously large (much larger than for other transitions to the region of positive energies) as a result of a substantial increase in the overlap integral between the wave functions. The absorption coefficient will accordingly increase in this region. The frequency of such transitions in real superlattices usually lies in the IR region.

As a parameter characterizing absorption per one electron in the ground state, we can conveniently use the square of the matrix element of the momentum operator, $p_n^2(k)$, for the transition between the states of the lowest and the n th excited miniband with equal Bloch vectors k (since the photon momentum is virtually zero, the transitions can be considered vertical). Derivatives such as the absorption cross section σ or the absorption coefficient α are proportional to p_n^2 .

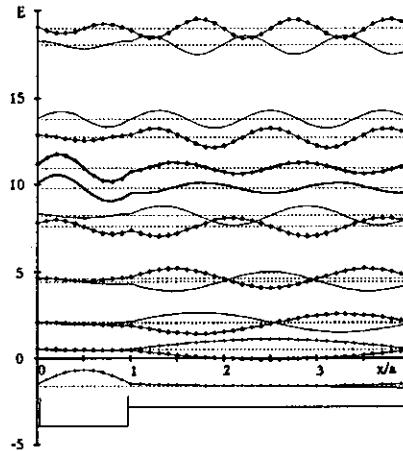


Fig. 2

Miniband superlattice structure at $b/a = 4$. Energy is given in $\hbar^2/(ma^2)$ units. The boundaries of minibands are shown by dashed lines. Solid lines are the wave functions at miniband boundaries, rhombs are the functions corresponding to $kb = 0$. Two thick curves are the wave functions of the "resonance" band. At the bottom, the structure potential is schematically shown.

The dependences of p_n^2 on the energy of the final state for two different superlattice periods are shown in Figs. 3 and 4. Variations of other parameters (a , Ω , V) do not qualitatively change the results. The figures show that the matrix element of the transition increases for a group of minibands in the resonance neighborhood. In each miniband, absorption is maximum at one boundary and almost vanishes at the other. This is characteristic of all minibands except for the resonance one. In the minibands with the energies lower than that of the resonance miniband, absorption monotonically decreases from bottom to top and, in the minibands lying above the resonance one, from top to bottom. A comparison with Fig. 2 shows that maximum absorption is observed when the wave function in the well has the "right" parity, i. e., opposite to that in the lowest miniband. In the resonance miniband, the parity of wave functions is "right" at both boundaries, so the corresponding absorption band has a different form.

The described pattern illustrates the hybrid character of the spectrum of the superlattice under consideration. Changes in the parity of states at the miniband boundaries after the transition through the resonance region is caused by "building in" of quasi-localized states in the well into the band structure formed by the main barriers.

When the distance between the wells increases, the transition matrix elements decrease; simultaneously, the miniband frequency increases. Therefore, absorption averaged over the energy range changes insignificantly.

Note that in a real superlattice, peaks corresponding to separate minibands may be diffuse largely because coherence of superlattice states deteriorates as a result of inevitable fluctuations of layer thicknesses, and the Bloch quasi-momentum k ceases to be a good quantum number. Some diffusion can be caused by different effective masses of electrons in the wells and barriers of the structure; we ignored this difference to simplify the calculations.

3. COMPARISON WITH THE ISOLATED WELL CHARACTERISTICS

In [6], analytic calculations of the electron and optical properties were performed for a heterostructure comprised of a solitary quantum well with model potential (1). Naturally, it could be expected that the results of our calculations should agree with those obtained in [6] in the limit of widely spaced wells; that is, in the limit of a long-period superlattice with $b/a \gg 1$.

The physical quantity characterizing optical absorption in an isolated quantum well per one carrier is $p_n^2 \rho$, where p_n^2 is the square of the momentum operator matrix element, and ρ is the density of final

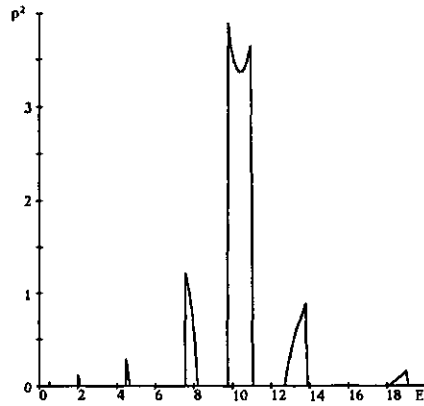


Fig. 3

Energy dependence of the square of the matrix element of momentum for the system corresponding to Fig. 2. Energy is plotted in $\hbar^2/(ma^2)$ units, and the square of the matrix element, in \hbar^2/a^2 .

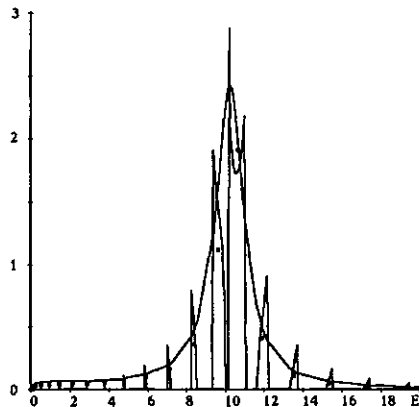


Fig. 4

The same dependence as in Fig. 3 at $b/a = 10$. Squares correspond to $\langle p_n^2 \rangle / (E_n - E_{n-1})$ ratios for the superlattice, that is, to matrix element values averaged over spectral intervals. Smooth curve is the product $p_n^2 \rho$ of the square of the momentum operator matrix element and the density of final states in an isolated quantum well according to [6].

electron states. For a superlattice, a similar parameter characterizing absorption per electron averaged over an energy range is $\langle p_n^2 \rangle / (E_n - E_{n-1})$ in the neighborhood of the n th miniband. Here, $\langle p_n^2 \rangle$ is the square of the matrix element averaged over the states of the n th miniband, and E_n is the energy at the middle of the miniband (at $kb = \pi/2$). Figure 4 shows that these two values are fairly close to each other even at $b/a = 10$.

CONCLUSIONS

To summarize, in a superlattice with resonance states in its unit cell, the mean dipole matrix element for transitions from the lowest to higher subbands noticeably increases for those finite subbands that lie in the neighborhood of the resonance. The increase is the more substantial the smaller the energy difference between the subband and the resonance. For all finite subbands except for the one closest to the resonance, the matrix element turns zero at one of the subband boundaries. The intersubband absorption coefficient of the superlattice, which can be calculated from the known matrix element in the same way as in [6], exhibits

a similar behavior. As concerns the shape of the absorption peak of the miniband closest to the resonance, it strongly depends on the incorporation of quasi-localized states into the spectrum.

This work was financially supported by the Russian Foundation for Basic Research (Grants 96-15-96500 and 97-02-17334).

REFERENCES

1. V.P. Kaidanov and Yu.I. Ravich, *Usp. Fiz. Nauk*, vol. 145, p. 51, 1985.
2. R.V. Pol', *Introduction to Optics* (in Russian), par. 122, Gostekhizdat, Moscow, 1947.
3. W. Heitler, *The Quantum Theory of Radiation*, Oxford, 1954.
4. S.D. Beneslavskii, A.V. Dmitriev, and N.S. Salimov, *Zh. Eksp. Teor. Fiz.*, vol. 92, p. 305, 1987.
5. A.V. Dmitriev, *Solid State Commun.*, vol. 74, p. 237, 1990.
6. A.V. Dmitriev, R. Keiper, and V.V. Makeev, *Semicond. Sci. Technol.*, vol. 11, p. 1791, 1996.
7. B.F. Levine, *J. Appl. Phys.*, vol. 74, p. R1, 1993.
8. G. Bastard, *Phys. Rev.*, vol. B24, p. 5693, 1981.
9. G. Bastard, *Phys. Rev.*, vol. B25, p. 7584, 1982.
10. Hung-Sik Cho and P.R. Prucnal, *Phys. Rev.*, vol. B36, p. 3237, 1987.

12 March 1999

Department of Low-Temperature Physics